Scripta Materialia 65 (2011) 245-248

Dilatometric analysis of cementite dissolution in hypereutectoid steels containing Cr

Jae-Yong Chae, Jae-Hoon Jang, Guohong Zhang, Kwan-Ho Kim[1], Jae Seung Lee[1], H.K.D.H. Bhadeshia and Dong-Woo Suh*

Graduate Institute of Ferrous Technology (GIFT), POSTECH, Pohang, 790-784, Korea
[1] Technical Research Laboratories, POSCO, Pohang, 790-785, Korea

Abstract

Cementite dissolution in hypereutectoid steels containing Cr is analyzed using dilatometry combined with the consideration of the carbon content in the austenite. The results suggest that the austenite transformed from the mixture of ferrite and cementite can be approximated to have a carbon content corresponding to equilibrium with ferrite. The overall dissolution behavior of cementite is described well with the suggested analysis procedure.

Keywords : dilatometry, cementite, hypereutectoid steels, bearings

*Corresponding author: Dong-Woo Suh
Email : dongwoo1@postech.ac.kr
Tel: +82-54-279-9030
Fax: +82-54-279-9299

There have been many studies on the phase transformation of steels based on analyzing the changes in a dimension of a test specimen using a technique designated dilatometry [1-5]. A partitioning of the observed transformation strain according to a lever rule relative to the pure parent and product phases is the simplest analysis [1], but more precise models employing the lattice parameters of the constituent phases and considering anisotropic volume changes have also been suggested [2-6]. Most of the dilatometric analyses have been developed for hypoeutectoid steels. The transformation strain during the isothermal decomposition of austenite in hypereutectoid steel was studied by Li et al. [7]. Recently Lee et al. also reported a dilatometric analysis of austenite formation in hypereutectoid steel, which focused on the early stage of cementite dissolution with an empirical consideration of the carbon concentration in austenite [8].

During the heating of hypereutectoid steel, all ferrite and some of the cementite transforms cooperatively into austenite (stage 1) and then the remainder of the carbide dissolves once the ferrite is all consumed (stage 2) [9]. The purpose of the present study was to examine the overall cementite dissolution kinetics upon heating of hypereutectoid steel using dilatometry. Two different assumptions regarding the carbon concentration in austenite during stage 1 are supposed and integrated into the dilatometric analysis. Metallographic analysis is conducted to confirm which condition reasonably describes the observed dissolution behavior of cementite in stage 1 as well as the validity of proposed analysis.

The chemical compositions of alloys A and B are 1.0C-0.35Mn-0.25Si-1.4Cr wt% and 1.0C-0.35Mn-1.25Si-1.4Cr wt%, respectively. Alloy A resembles the composition of SAE52100 steel used in the manufacture of bearings. The alloys were prepared using vacuum-induction melting and hot-rolling. After a spheroidizing heat-treatment, the initial microstructure consists of a ferrite matrix and spheroidized cementite. Cylindrical dilatometric samples 3 mm diameter and 10 mm length were heated to 1100^{o}C at a heating rate of 1^{o}C s^{-1} to monitor the length change. Interrupted quenching was employed to freeze the microstructure as a function of temperature for metallographic analysis. Scanning electron microscopy was used on samples etched with a 2% nital solution. The fraction of cementite was measured using a point-counting method [10].

Fig. 1 shows the transformation strains of alloys A and B as observed during heating. The deviation of dilatometric curves from linear behavior marked as ‘1’ corresponds to the formation of austenite from the original mixture of ferrite and cementite. The non-linear behavior in the temperature interval where the specimen length increases again, marked as ‘2’, is reported to originate from the cementite dissolution in austenite matrix [7].

A sequential process of stage 1 and 2 upon heating is assumed for analysis of phase fraction

from dilatometric curves. Dilatometric analysis in stage 1 deals with the fractions of ferrite (α), cementite (θ) and austenite (γ). The average atomic volume (V) of the sample is,

$$\begin{aligned} V &= f_\alpha \cdot V_\alpha + f_\theta \cdot V_\theta + f_\gamma \cdot V_\gamma \\ &= (V_\alpha - V_\gamma)\cdot f_\alpha + (V_\theta - V_\gamma)\cdot f_\theta + V_\gamma \end{aligned} \quad (1)$$

Here, V_i is average atomic volume of an atom in the ith-phase, f_i is the volume fraction of the ith-phase. The temperature dependence of the average atomic volume of ferrite and cementite is evaluated from the lattice parameters in Table 1 [11-15]. It is noted that the lattice parameters in Table 1 do not consider the effect of alloying elements other than carbon, therefore, even with a considerable enrichment of Cr in cementite, the influence on the atomic volume is assumed to be negligible. Since the average atomic volume of sample, V, can be derived from dilatometric data, Eq. (1) contains three unknowns, f_α, f_θ and the carbon concentration in austenite.

Ignoring the small concentration of carbon in ferrite, a mass balance for carbon gives,

$$C_0 = \frac{C_\theta \rho_\theta f_\theta + C_\gamma \rho_\gamma f_\gamma}{\rho_\alpha f_\alpha + \rho_\theta f_\theta + \rho_\gamma f_\gamma} \quad (2)$$

Here, C_i represents a weight fraction of carbon in the ith-phase. ρ_i, the density of the ith-phase is expressed as follows:

$$\rho_\alpha = \frac{M_{Fe}}{V_\alpha} \quad , \quad \rho_\theta = \frac{12M_{Fe} + 4M_C}{12V_\theta} \quad , \quad \rho_\gamma = \frac{M_{Fe} + \left(\frac{X_C}{1 - X_C}\right)M_C}{V_\gamma} \quad (3)$$

Here, M_{Fe} and M_C are atomic weights of Fe and C, and X_C is atomic fraction of carbon in austenite. Rearranging Eq. (2) gives,

$$f_\theta = A \cdot f_\alpha + B \quad (4)$$

$$A = \frac{[C_0(\rho_\alpha - \rho_\gamma) + C_\gamma \rho_\gamma]}{[(C_\theta \rho_\theta - C_\gamma \rho_\gamma - C_0(\rho_\theta - \rho_\gamma)]}, \quad B = \frac{(C_0 \rho_\gamma - C_\gamma \rho_\gamma)}{[(C_\theta \rho_\theta - C_\gamma \rho_\gamma - C_0(\rho_\theta - \rho_\gamma)]}$$

Eqs. (1) and (4) offer two relations among f_α, f_θ and the carbon concentration in austenite, but there are no more deterministic conditions. In the previous works on the dilatometric analysis of hypoeutectoid steels of which microstrucuture consisted of ferrite and pearlite, it was assumed that the austenite inherits the carbon concentration of pearlite until cementite completely dissolves in austenite [16-17]. Under that condition, the carbon concentration in the austenite is treated as a constant determined by the initial cementite fraction in pearlite. However, it is not clear that such an assumption is still applicable to austenitization of a hypereutectoid steel where the starting microstructure contains cementite in spheroidized form.

Fig. 2(a) shows a schematic diagram on the formation of austenite from ferrite and spheroidized cementite. For the growth of austenite, dissolved cementite should supply the austenite with carbon which diffuses to the ferrite/austenite interface. The carbon level in the austenite side of the interface is given by the equilibrium between the ferrite and austenite. In high carbon steels, Cr has to be redistributed during dissolution of cementite below a critical temperature which corresponds to the kinetic boundary associated with the partitioning of Cr [9]. With the Cr partitioning, the activity of carbon at the austenite/cementite interface is increased to be equivalent to that at the ferrite/austenite interface [9]. In this case, the average carbon concentration in austenite can be approximated to that of austenite in local equilibrium with ferrite.

In the present study, following two assumptions are considered on the carbon concentration in austenite and combined with the dilatometric analysis:

(i) carbon content of austenite maintaining the local equilibrium with ferrite at the interface, $C^{\gamma\alpha}$

(ii) a constant carbon content corresponding to equilibrium cementite fraction in pearlite, $C^{pearlite}$

Comparison of the dilatometry results with the metallographic observations shows which condition will prevail.

Fig. 2(b) shows the change of $C^{\gamma\alpha}$ and $C^{pearlite}$ as a function of temperature in Fe-1.0C-1.4Cr system. The calculations were performed with the TCFE6 database of Thermo-Calc software. As the temperature increases, the carbon content in austenite for local equilibrium with ferrite decreases rapidly compared with the constant carbon level of $C^{pearlite}$. This indicates that the assumption regarding to the carbon content in austenite will significantly affect the results of dilatometric analysis.

Meanwhile, in stage 2 where f_α is zero, the average atomic volume is expressed as,

$$V = f_\theta \cdot V_\theta + f_\gamma \cdot V_\gamma = V_\theta + (V_\gamma - V_\theta) \cdot f_\gamma \quad (5)$$

From a mass balance with respect to carbon,

$$f_\gamma = \frac{(C_\theta - C_0) \cdot \rho_\theta}{[(C_0 - C_\gamma) \cdot \rho_\gamma - (C_0 - C_\theta) \cdot \rho_\theta]} \quad (6)$$

Combining (5) and (6) yields a non-linear equation of the carbon content in austenite which will give the phase fraction of cementite and austenite at a given temperature.

Fig. 3(a) shows results of dilatometric analysis of alloy A coupled with each assumption on the carbon content in austenite during the stage 1. It shows that about 30% of initial cementite will dissolve in austenite when assuming that austenite has the carbon content corresponding to the local equilibrium with ferrite, $C^{\gamma\alpha}$. On the other hand, over 60% of spheroidized cementite is supposed to dissolve in austenite during stage 1 with $C^{pearlite}$ assumption. Fig. 3(b) shows SEM images of interrupted quenched samples. It is noted that pearlitic cementite appears after quenching from 800^{o}C as marked with the arrows. This pearlitic cementite is believed to evolve from austenite during interrupted quenching, so its fraction is not included in the metallographic analysis. The symbols in Fig. 3(a) represent the metallographic analysis of the cementite fraction. Approximately 18% of cementite is found to dissolve. It suggests that the dilatometric analysis with $C^{\gamma\alpha}$ assumption might reflect better the real situation. Recently, the cementite dissolution with Cr partitioning at 800^{o}C was experimentally confirmed in 0.6C-1.0Cr steel and it was reported that the cementite could be dissolved without Cr partitioning above 880^{o}C [18]. The temperature is calculated to be 875^{o}C in 1.0C-1.4Cr steel in the present study. Given that the temperature range of stage 1 is approximately 750~800^{o}C, the cementite dissolution to form austenite should be accompanied by the partitioning of Cr, which is consistent with the assumption on the carbon concentration of $C^{\gamma\alpha}$. Figs. 4 (a) and (b) show the change of phase fraction in overall temperature interval with $C^{\gamma\alpha}$ assumption for the dilatometric analysis of stage 1. Analysis results of cementite dissolution shows excellent agreements with the metallographic ones for both alloys A and B. It suggests that proposed dilatometric procedure gives a reliable analysis on cementite dissolution as well as change of phase fraction in hypereutectoid steels containing Cr. However, it is noted that a separated investigation is needed whether $C^{\gamma\alpha}$ assumption will still be valid when the alloy does not contain substitutional elements requiring partitioning during cementite dissolution.

In summary, observations of transformation strain during the formation of austenite as a mixture of ferrite and spheroidized cementite is heated cannot be fully interpreted without a knowledge of the carbon concentration in the austenite. An analysis of the results indicates that the concentration to use is that which places the growing phase in equilibrium with the ferrite. An alternative scenario where the growing austenite inherits the average composition of pearlite is shown not to be viable.

This research was supported by WCU(World Class University) program through the National Research Foundation of Korea funded by the Ministry of Education, Science and Technology (R32-10147).

References

[1] ASTM Standard A1033-10, ASTM International, West Conshohocken, PA, 2010.
[2] T. A. Kop, J. Sietsma, S. Van Der Zwaag: J. Mat. Sci. 36 (2001) 519-526.
[3] C. Garcia-Mateo, F. G. Caballero, C. Capdevila, C. G. Andres: Scripta Mater. 61 (2009) 855-858.
[4] S. Choi: Mat. Sci. & Eng. A 363 (2003) 72-80.
[5] D. W. Suh, C. S. Oh, H. N. Han, S. J. Kim: Acta Mater. 55 (2007) 2659-2669.
[6] A. Matsuzaki, H. K. D. H. Bhadeshia: Acta Metall. & Mater. 42 (1994) 1081-1090.
[7] C. M. Li, F. Sommer, E. J. Mittemeijer: Z. Metallkd. 92 (2001) 32-36.
[8] S. J. Lee, K. D. Clarke: Metall. & Mater. Trans. A 41 (2010) 3027-3031.
[9] M. Hilert, K. Nilsson, L. E. Törndahl: JISI 209 (1971) 49-66.
[10] ASTM Standard E562-08, ASTM International, West Conshohocken, PA, 2008.
[11] M. Onink, F. D. Tichelaar, C. M. Brakman, E. J. Tittemeijer, S. Van Der Zwaag: Z. Metall. 87 (1996) 24-32.
[12] H. Stuart, N. Ridley: JISI, 204 (1966) 711-717.
[13] M. Onink, D. Tichelaar, M. Brakman, J. Mittemeijer, S. Van Der Zwaag, J. H. Root, N. B. Konyer: Scripta Metall. Mater. 29 (1993) 1011-1016.
[14] C. Qiu, S. Van Der Zwaag: Steel Res. 68 (1997) 32-38.
[15] R. C. Reed, J. H. Root: Scripta Mater. 38 (1997) 95-99.
[16] D. W. Suh, C. S. Oh, S. J. Kim: Met. & Mater. Int. 14 (2008) 275-282.
[17] S. J. Lee, K. D. Clarke, C. J. Van Tyne: Metall. & Mater. Trans. A 41 (2010) 2224-2235.
[18] G. Miyamoto, H. Usuki, Z. D. Li, T. Furuhara: 58 (2010) 4492-4502.

Table 1. Lattice parameters of austenite, ferrite and cementite [11-15]

	Lattice parameter in Å
austenite	$a_\gamma=(3.6306+0.78\cdot C_\gamma)\cdot\{1+(24.9-50\cdot X_\gamma)\cdot 10^{-6}\cdot(T-1000)\}$
ferrite	$a_\alpha=2.8863\cdot\{1+17.5\cdot 10^{-6}\cdot(T-800)\}$
cementite	$a_\theta=4.5234\cdot\{1+(5.311\cdot 10^{-6}-1.942\cdot 10^{-9}\cdot T+9.655\cdot 10^{-12}\cdot T^2)\cdot(T-293)\}$ $b_\theta=5.0883\cdot\{1+(5.311\cdot 10^{-6}-1.942\cdot 10^{-9}\cdot T+9.655\cdot 10^{-12}\cdot T^2)\cdot(T-293)\}$ $c_\theta=6.7426\cdot\{1+(5.311\cdot 10^{-6}-1.942\cdot 10^{-9}\cdot T+9.655\cdot 10^{-12}\cdot T^2)\cdot(T-293)\}$

(X_γ is atomic fraction of solute carbon in austenite and T is in K)

Fig. 1 Dilatometric curves of alloys A and B on heating

Fig. 2 (a) Schematic description of diffusion of carbon for austenite formation from mixture of ferrite and cementite and (b) weight fraction of carbon in austenite according to each condition

Fig. 3(a) Dilatometric analysis results with $C^{\gamma\alpha}$ and $C^{pearlite}$ assumptions and (b) SEM micrographs of interrupted quenched alloy A

Fig. 4 Change of phase fraction using dilatometry of (a) alloy A and (b) alloy B. Symbols represent the cementite fraction with metallographic analysis

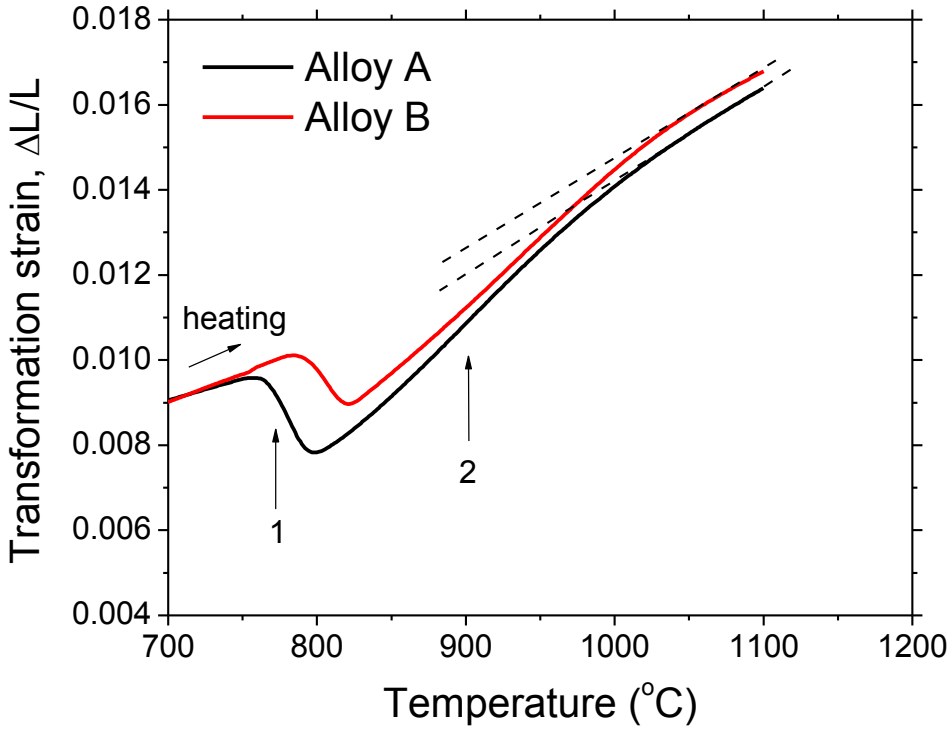
Alloy A
Alloy B
heating
1
2
Transformation strain, ΔL/L
Temperature (°C)
0.018
0.016
0.014
0.012
0.010
0.008
0.006
0.004
700
800
900
1000
1100
1200

Fig. 1

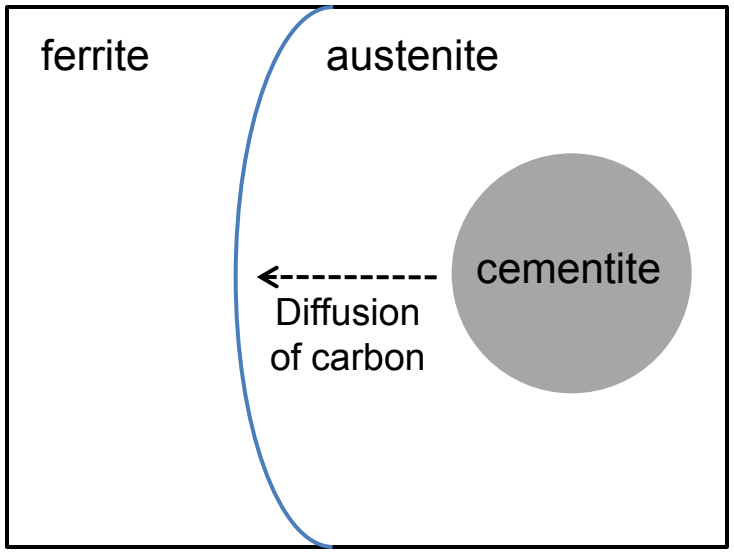
ferrite
austenite
cementite
Diffusion
of carbon

(a)

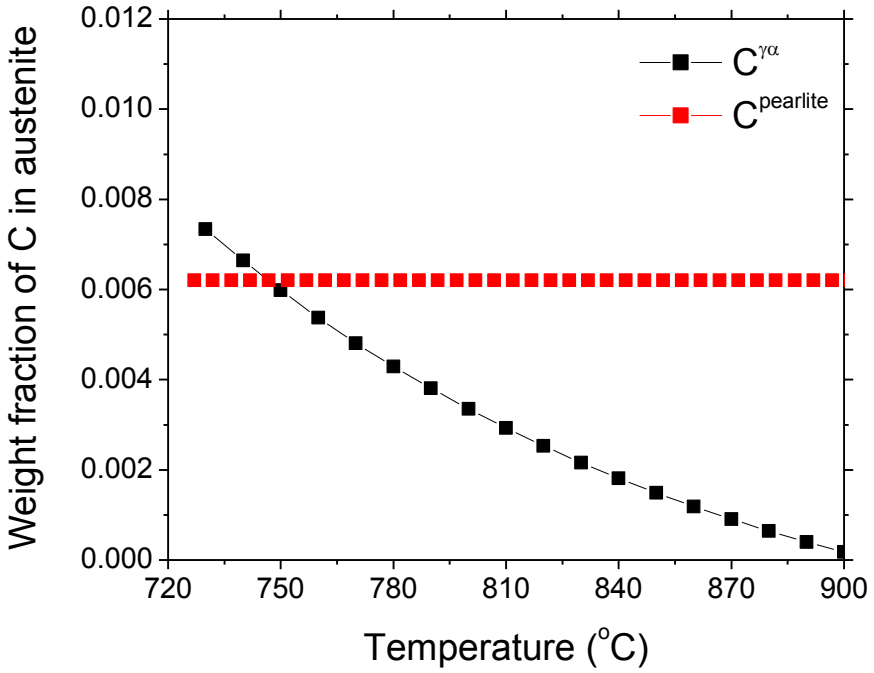
Weight fraction of C in austenite
0.012
0.010
0.008
0.006
0.004
0.002
0.000
720
750
780
810
840
870
900
Temperature (°C)
C^γα
C^pearlite

(b)

Fig. 2

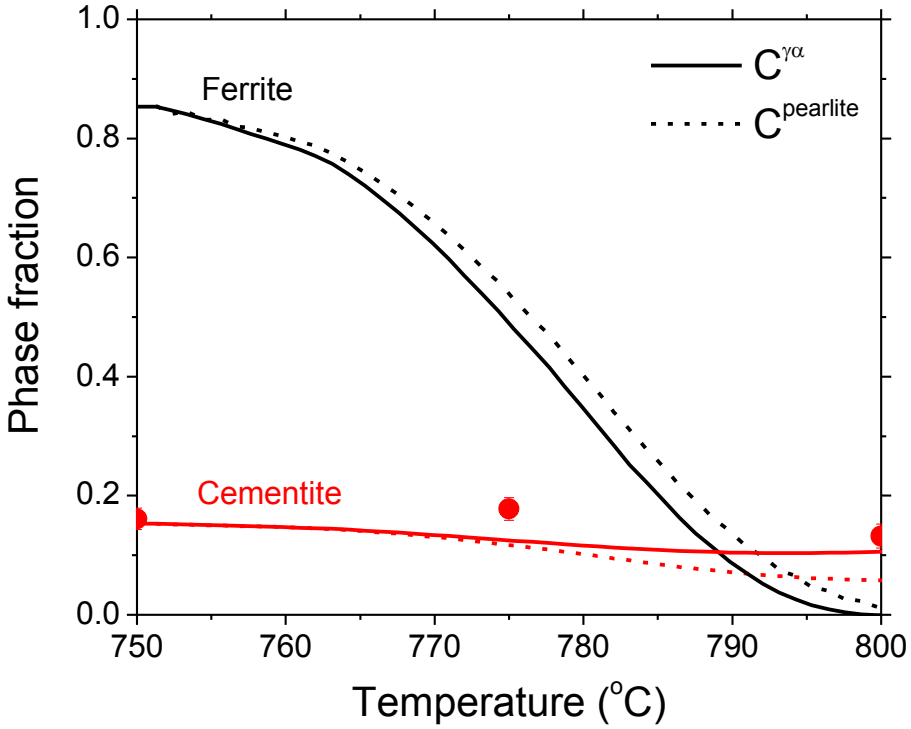
1.0
0.8
0.6
0.4
0.2
0.0
Phase fraction
Ferrite
Cementite
$C^{\gamma\alpha}$
$C^{pearlite}$
750
760
770
780
790
800
Temperature (°C)

(a)

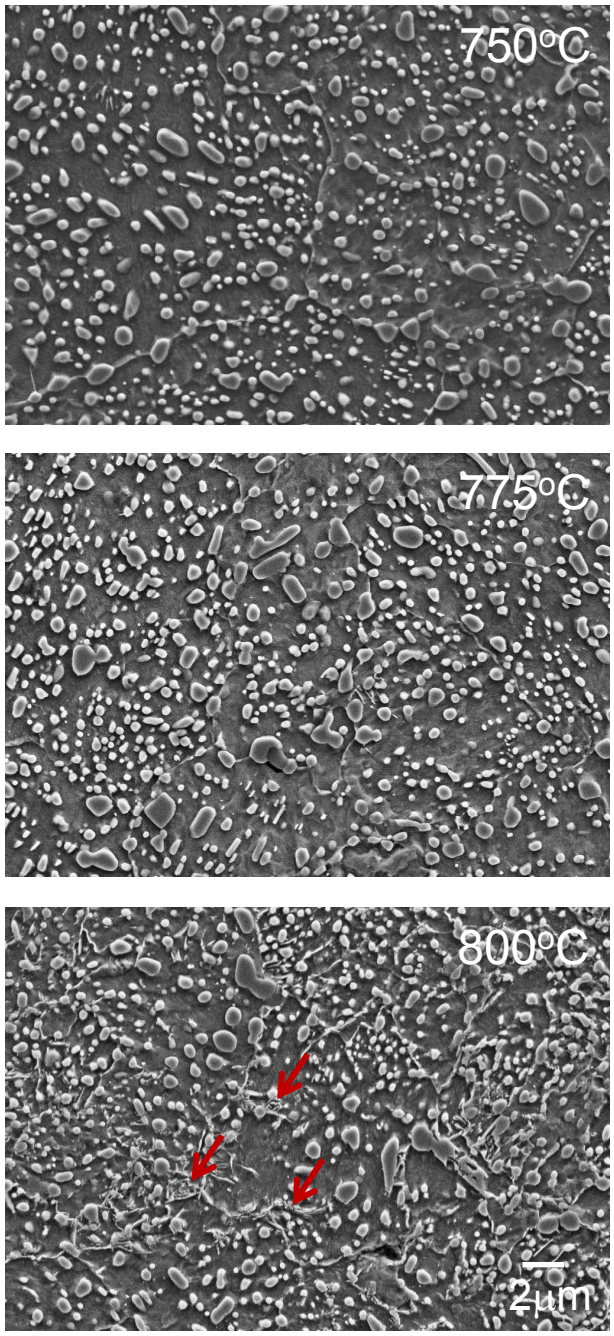
750°C
775°C
800°C
2μm

(b)

Fig. 3

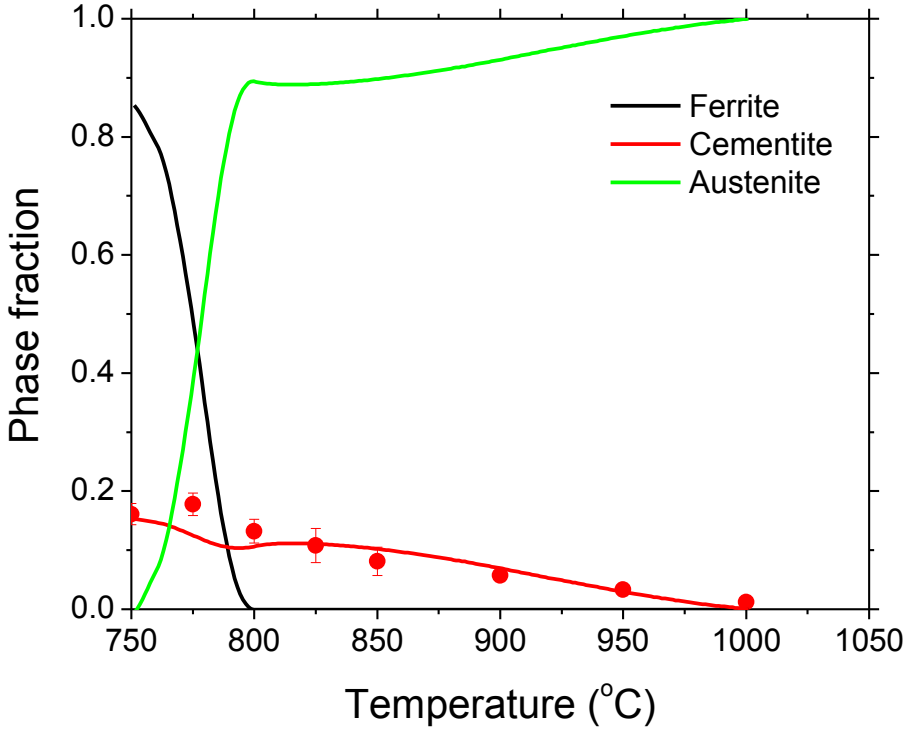
Phase fraction
Temperature (°C)
Ferrite
Cementite
Austenite
1.0
0.8
0.6
0.4
0.2
0.0
750
800
850
900
950
1000
1050

(a)

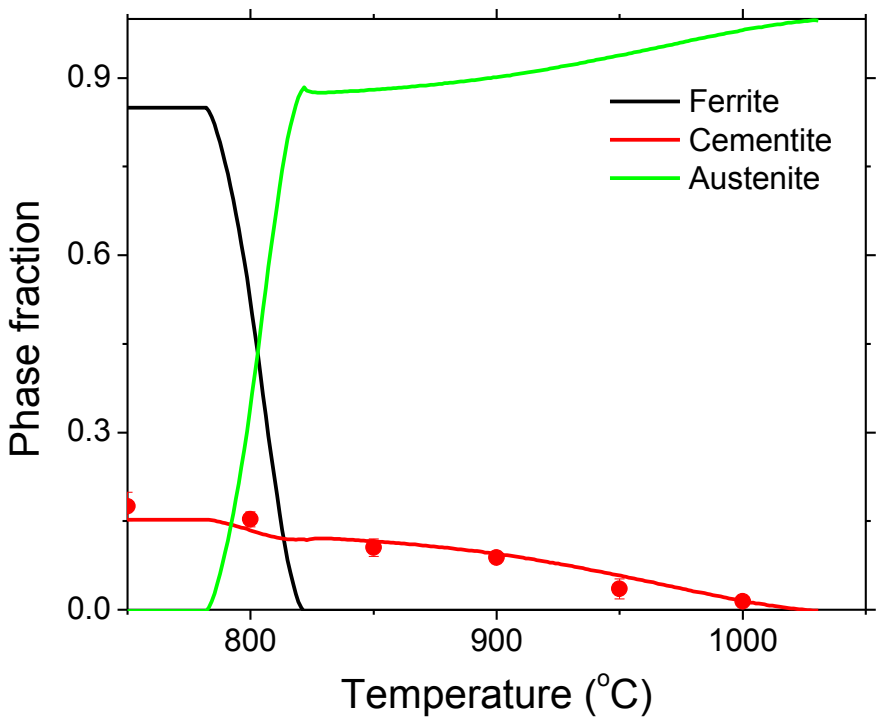
Phase fraction
Temperature (°C)
Ferrite
Cementite
Austenite
0.9
0.6
0.3
0.0
800
900
1000

(b)

Fig. 4